Abstract. This article explores the role of numerical optimization methods in the development of artificial intelligence systems. A comparative analysis of three widely used methods – SGD, AdamW, and mL-BFGS – is conducted. The paper examines the mathematical framework of each algorithm, the principles of working with first- and second-order gradients, and adaptability strategies. Particular attention is paid to stabilization mechanisms for approximating the Hessian matrix under stochastic noise conditions. The presented testing results confirm the effectiveness of second-order methods in accelerating model convergence.

Keywords: Numerical optimization, gradient descent, AdamW, mL-BFGS, Hessian matrix, convergence, neural networks.

СПИСОК ВИКОРИСТАНОЇ ЛІТЕРАТУРИ

1. Чисельні методи: навчальний посібник / Л. О. Волонтир, О. В. Зелінська, Н. А. Потапова, І. А. Чіков. Вінниця: ВНАУ, 2020. 322 с. URL: https://r.donnu.edu.ua/handle/123456789/1805

2. Bottou L., Curtis F., Nocedal J. Optimization Methods for Large-Scale Machine Learning. *https://epubs.siam.org/doi/10.1137/16M1080173*. URL: https://epubs.siam.org/doi/10.1137/16M1080173 (дата звернення: 11.03.2026).

3. Rafati J., Roummel F. M. Quasi-Newton Optimization Methods For Deep LearningApplications. *https://arxiv.org/abs/1909.01994*. URL: https://arxiv.org/abs/1909.01994 (дата звернення: 11.03.2026).

4. mL-BFGS: A Momentum-based L-BFGS for Distributed Large-Scale Neural Network Optimization – PMC. *PMC*. URL: https://pmc.ncbi.nlm.nih.gov/articles/PMC12393816/ (дата звернення: 18.03.2026).

5. Venues | OpenReview. URL: https://openreview.net/pdf/5963886abef941684ffc0cf670297e47fb1e5155.pdf (дата звернення: 18.03.2026).

6. Niu Y. mL-BFGS: A Momentum-based L-BFGS for Distributed Large-Scale Neural Network Optimization. *researchgate*. URL: https://www.researchgate.net/publication/372654300_mL-BFGS_A_Momentum-based_L-BFGS_for_Distributed_Large-Scale_Neural_Network_Optimization (дата звернення: 19.03.2026).

UDC 528.8:581.5(477.44)

SPATIOTEMPORAL DYNAMICS OF KNDVI IN VINNYTSIA CITY DURING THE VEGETATION GROWING SEASON: TREND ANALYSIS FOR 1990–2021

A. O. Chernenko, A. M. Mischenko

Summary. This study examines the spatiotemporal dynamics of urban vegetation in Vinnytsia over a 32-year period (1990–2021) using the Kernel Normalized Difference Vegetation Index (KNDVI) derived from Landsat satellite imagery within the Google Earth Engine (GEE) environment. Annual composite KNDVI maps were generated for the vegetation growing season (May–September) and analysed using pixel-wise linear regression to quantify interannual trends. To capture potential shifts in vegetation dynamics, the analysis was conducted separately for two sub-periods: 1990–2005 and 2005–2021. The results indicate a substantial increase in the proportion of statistically significant positive trends in the latter period, with the dominant pattern shifting from mixed (34.435 negative, 66.575 positive) to strongly positive (11.705 negative, 88.305 positive), suggesting pronounced urban greening. The fully scripted Python/GEE workflow provides a reproducible and scalable alternative to conventional desktop GIS approaches for long-term urban vegetation monitoring.

Keywords: KNDVI, urban vegetation, spatiotemporal analysis, Google Earth Engine, Vinnytsia.

Introduction. Urban vegetation provides a wide range of ecosystem services, including mitigation of the urban heat island effect, regulation of stormwater runoff, carbon sequestration, improvement of air quality, and support of biodiversity and human well-being [1; 2]. As urban areas continue to expand, the ability to monitor vegetation extent and condition at high spatial and temporal resolution becomes increasingly important for evidence-based urban planning and environmental management.

Remote sensing offers a cost-effective and spatially explicit approach for assessing vegetation dynamics over large areas and extended time periods [3]. Vegetation indices derived from multispectral satellite imagery–most notably the Normalized Difference Vegetation Index (NDVI)–have been widely used to monitor phenological dynamics, detect land-cover change, and quantify vegetation responses to climatic variability [4; 3]. However, NDVI is known to saturate in dense canopies and to be sensitive to soil background reflectance, which can limit its performance in heterogeneous urban landscapes [3; 5].

The Kernel Normalized Difference Vegetation Index (KNDVI), introduced by Camps-Valls et al. [5], addresses these limitations by embedding NDVI within a radial basis function kernel. This

formulation yields a bounded and more sensitive index, particularly at high vegetation densities, while improving robustness to background effects [5].

Long-term, city-scale analyses of vegetation dynamics remain relatively scarce in the Ukrainian context. Vinnytsia–a mid-sized city (approximately 370,000 inhabitants) in central Ukraine, characterised by an extensive network of urban parks, street trees, and riparian forest belts along the Southern Bug–provides a valuable case study. Understanding how its vegetation cover has evolved over the past three decades, and whether these trends exhibit temporal shifts, is directly relevant to urban ecology and the planning of green infrastructure.

Materials and Methods. The study area corresponds to the administrative boundary of Vinnytsia (approximately 130 km²), located at 49.23°N, 28.47°E within the forest-steppe zone of central Ukraine. Annual KNDVI maps were derived from Landsat Collection 2 Level-2 surface reflectance products. To ensure radiometric consistency across the 32-year study period, sensor transitions were handled as follows: Landsat 4 TM combined with Landsat 5 TM (1990–1998); Landsat 5 TM combined with Landsat 7 ETM+ prior to the scan-line corrector (SLC) failure (1999–2002); Landsat 5 TM only (2003–2012), thereby avoiding SLC-off artefacts in ETM+ imagery acquired after May 2003; and Landsat 8 OLI (2013–2021). For each year, imagery was restricted to the May–September growing season and filtered using a scene-level cloud-cover threshold of 80%.

The May–September window was selected to encompass the full snow-free phenological cycle characteristic of the temperate continental climate of central Ukraine, including spring green-up (May), peak biomass (June–August), and early senescence (September). Excluding April minimizes contamination from residual snowmelt, while inclusion of September allows the capture of late-season vegetation dynamics, including potential drought stress responses.

All preprocessing was performed in Google Earth Engine using the Python API. Pixel-level cloud and cloud-shadow masking were applied using the QA_PIXEL band (bits 3 and 4 corresponding to cloud and cloud shadow, respectively). Annual composites were generated using the median reducer across all valid observations within the growing season. The median statistic was selected for its robustness to residual cloud contamination and other anomalous reflectance values that can produce extreme index outliers.

For each annual composite, the per-pixel number of valid (cloud-free) observations was recorded as a quality metric. The number of images contributing to annual composites ranged from 5 to 18, depending on year and sensor availability.

Trend analysis was conducted post-export in Python using NumPy, SciPy, and Rasterio. For each of two sub-periods–1990–2005 ($n = 16$) and 2005–2021 ($n = 17$) – an ordinary least squares (OLS) linear regression was fitted independently at each pixel [6]:

$$KNDVI(t) = \beta_0 + \beta_1 \cdot t + \varepsilon,$$

where t denotes calendar year;

β_1 represents the slope ($\Delta KNDVI\ yr^{-1}$);

ε is the residual error term.

Statistical significance of the slope was assessed using a two-tailed *t*-test ($H_0: \beta_1 = 0; df = n - 2$), with a significance threshold of $p < 0.05$, following Li et al. [6]. Pixels with fewer than two valid observations were excluded from the analysis.

Significant trends were classified as positive ($\beta_1 > 0$; greening), negative ($\beta_1 < 0$; browning), or stable ($|\beta_1| \leq 10^{-3}$). In addition, maps of the coefficient of determination (R^2) were generated to evaluate model fit [6]. To characterise the aggregate temporal trajectory, the city-wide median KNDVI was calculated annually across all valid pixels.

Results. Table 1 summarises the pixel-wise regression statistics for both sub-periods. The proportion of pixels exhibiting statistically significant trends increased substantially from 30.45 to 59.65, corresponding to an increase in absolute count from 59,381 to 116,443 pixels. Importantly, the nature of these trends also shifted. During 1990–2005, 34.45 of significant pixels showed browning and 65.65 greening trends (approximately a 1:2 ratio). In contrast, during 2005–2021, greening trends became strongly dominant, accounting for 88.35 of significant pixels (approximately a 1:8 ratio).

Table 1

Summary of pixel-wise KNDVI linear trend statistics by sub-period

Period	Pixels with $p < 0.05$	No. of significant pixels	Negative trend (%)	Positive trend (%)
1990–2005	30.415	59,381	34.435	65.575
2005–2021	59.645	116,443	11.705	88.305

Figure 1 presents the annual time series of city-wide median KNDVI for Vinnytsia. Four broad temporal phases can be distinguished: (1) a relatively stable, oscillatory regime from 1990 to approximately 2000, with no clear directional trend; (2) a period of elevated but stable values from 2000 to 2004; (3) a pronounced decline from 2005 to 2011, during which all annual values remained below the long-term mean; and (4) a recovery and growth phase from 2012 to 2021, culminating in the highest recorded median value (0.367) in 2021. This temporal structure provides essential context for interpreting the regression-based trend estimates.

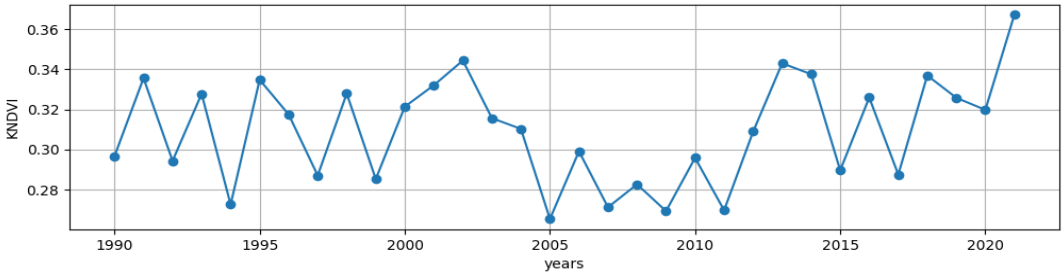

Figure 1. Annual city-wide median KNDVI for Vinnytsia
during the vegetation growing season (May–September), 1990–2021

Figure 2 shows the spatial distribution of statistically significant ($p < 0.05$) KNDVI trends for both sub-periods. In 1990–2005, significant trends are relatively sparse and spatially heterogeneous, with a mixed distribution of positive and negative slopes. In contrast, the 2005–2021 period is characterised by a markedly higher density of significant pixels and a clear predominance of positive trends. These greening trends are spatially concentrated in forested and park-dominated areas, particularly along the urban periphery and riparian zones.

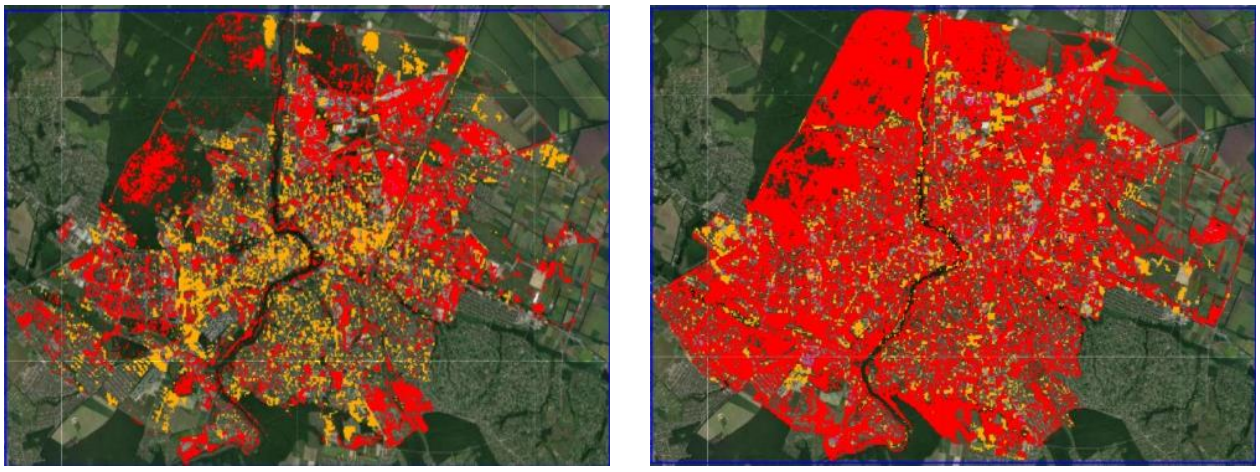

Figure 2. Spatial distribution of statistically significant KNDVI trends ($p < 0.05$)
for 1990–2005 (left) and 2005–2021 (right). Red: positive (greening); yellow: negative (browning);
purple: stable ($|\text{slope}| \leq 10^{-3}$).

Figure 3 presents the frequency distributions of significant slope values for both sub-periods. In both cases, the distributions are bimodal, with peaks centred around approximately −0.005 and +0.005 KNDVI yr^{-1}, and an overall range of approximately −0.02 to +0.02 KNDVI yr^{-1}. However, the relative prominence of these peaks differs markedly between periods. In 1990–2005, the positive

peak (~10,000 pixels) exceeds the negative peak (~4,000 pixels), whereas in 2005–2021 the positive peak (~20,000 pixels) becomes substantially more pronounced, while the negative peak declines (~2,000 pixels).

The patterns observed in Figures 2 and 3 can be interpreted in relation to the temporal phases identified in Figure 1. The first sub-period (1990–2005) primarily reflects phases (1) and (2), characterised by oscillatory dynamics and modest increases, resulting in weak and spatially heterogeneous trends. In contrast, the second sub-period (2005–2021) captures phases (3) and (4), comprising a pronounced decline followed by strong recovery. Although both sub-periods exhibit an overall upward trajectory, the magnitude of change is substantially greater in the latter period. The contrast between the depressed values of 2005–2011 and the elevated values after 2012 generates stronger positive slopes, explaining both the pronounced asymmetry in the slope distribution and the dominance of greening trends in the spatial maps.

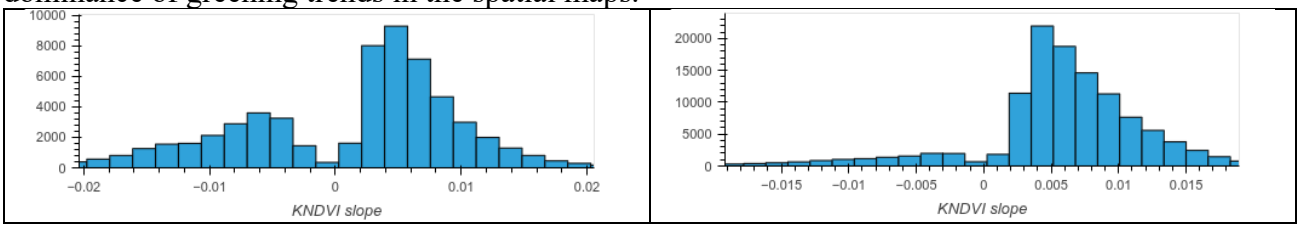

Figure 3. Frequency distributions of statistically significant KNDVI slope values (KNDVI yr^{-1}) for 1990–2005 (left) and 2005–2021 (right)

Conclusions. Pixel-wise linear trend analysis of KNDVI derived from multi-sensor Landsat time series provides a robust characterisation of long-term urban vegetation dynamics in Vinnytsia. The results reveal a clear structural shift from a period of weak, spatially limited trends (1990–2005) to a phase of strong and spatially extensive greening (2005–2021), associated with a transition in city-wide vegetation dynamics around 2005–2011.

The spatial concentration of greening trends within forested riparian corridors and peripheral park zones suggests that the observed increase in vegetation greenness is primarily driven by canopy maturation and densification of existing green infrastructure, rather than by expansion of vegetated areas within densely built-up zones. This distinction has important implications for urban planning, indicating that continued greening depends on the conservation and management of established forest stands, which remain vulnerable to land-use change and climatic extremes.

The application of KNDVI, as opposed to conventional NDVI, is advantageous in this context due to its reduced saturation in dense canopies and improved sensitivity to vegetation structure, making it more suitable for heterogeneous urban environments [6].

The Google Earth Engine–Python workflow developed in this study offers significant advantages in terms of reproducibility, scalability, and computational efficiency compared to traditional desktop GIS approaches. The fully cloud-based processing pipeline–from image filtering and masking to compositing and export–can be readily extended to additional vegetation and urban indices (e.g., EVI, NDBI, land surface temperature) and applied to other cities or longer time series with minimal modification.

Future work will integrate climatic reanalysis data (e.g., ERA5 temperature and precipitation anomalies) to disentangle the relative contributions of climate variability and land-use change to the observed vegetation dynamics. In addition, expanding the analysis to multiple urban indices will enable assessment of the spatial coupling between vegetation change and urban heat island intensity.

Анотація. У дослідженні розглянуто просторово-часову динаміку міської рослинності у Вінниці протягом 32-річного періоду (1990–2021) з використанням Kernel Normalized Difference Vegetation Index (KNDVI), розрахованого на основі супутникових знімків Landsat у середовищі Google Earth Engine (GEE). Щорічні композитні карти KNDVI були створені для вегетаційного періоду (травень–вересень) та проаналізовані за допомогою попіксельної лінійної регресії для кількісної оцінки міжрічних трендів. Для виявлення можливих змін у динаміці рослинності аналіз проводився окремо для двох підперіодів: 1990–2005 і 2005–2021. Результати свідчать про суттєве зростання частки статистично значущих позитивних трендів у пізнішому періоді, причому

домінуючий характер змін змінився зі змішаного (34,435 негативних; 66,575 позитивних) на виражено позитивний (11,705 негативних; 88,305 позитивних), що вказує на помітне озеленення міського середовища. Повністю скриптований робочий процес Python/GEE забезпечує відтворювану та масштабовану альтернативу традиційним підходам настільних ГІС для довготривалого моніторингу міської рослинності.

Ключові слова: KNDVI, міська рослинність, просторово-часовий аналіз, Google Earth Engine, Вінниця.

REFERENCES

1. Zhang, Y., Zhang, X., Liu, S., & Cai, W. (2022). Spatiotemporal variation of vegetation NDVI and its climatic driving forces in global land surface. *Polish Journal of Environmental Studies,* 31(4), 3541–3549. https://doi.org/10.15244/pjoes/145063

2. Nowak, D. J., & Crane, D. E. (2002). Carbon storage and sequestration by urban trees in the USA. *Environmental Pollution,* 116(3), 381–389.

3. Pettorelli, N., Vik, J. O., Mysterud, A., Gaillard, J.-M., Tucker, C. J., & Stenseth, N. C. (2005). Using the satellite-derived NDVI to assess ecological responses to environmental change. *Trends in Ecology & Evolution,* 20(9), 503–510.

4. Tucker, C. J. (1979). Red and photographic infrared linear combinations for monitoring vegetation. *Remote Sensing of Environment,* 8(2), 127–150.

5. Camps-Valls, G., Campos-Taberner, M., Moreno-Martínez, Á., Walther, S., Duveiller, G., Cescatti, A., Mahecha, M. D., Muñoz-Marí, J., García-Haro, F. J., Guanter, L., Jung, M., Gamon, J. A., Reichstein, M., & Running, S. W. (2021). A unified vegetation index for quantifying the terrestrial biosphere. *Science Advances,* 7(9), eabc7447

6. Li, X., Wang, L., Geng, X., & Zhou, W. (2022). Spatiotemporal variation of vegetation NDVI and its climatic driving forces in global land surface. *Polish Journal of Environmental Studies,* 31(4), 3541–3549.

UDC 504.064:591.5:598.2(7)

TEMPORAL TRENDS IN BREEDING BIRD DIVERSITY ACROSS NORTH AMERICA: A LINEAR MIXED-EFFECTS MODEL ANALYSIS

O. S. Mozharovskyi, A. M. Mishchenko

Summary. Long-term biodiversity monitoring data require analytical frameworks that can simultaneously capture continental-scale trends and local variation. We applied linear mixed-effects models (LMMs) to data from the North American Breeding Bird Survey (BBS) spanning 440 survey routes and 24 years (1984–2007) to assess temporal trends in six biodiversity indices – species richness (S), total abundance (N), Shannon entropy (H), and Simpson-based indices (D, 1−D, 1/D) – and to evaluate whether climate (temperature, precipitation) and vegetation (NDVI) can account for the observed trends. Fixed effects in LMMs estimate trends in mean local (alpha) diversity, while random effects quantify heterogeneity among locations (beta diversity). All biodiversity indices showed statistically significant directional trends over the study period. Species richness, Shannon entropy, and evenness-related indices increased moderately, while total abundance declined. Intraclass correlation coefficients (ICC = 0.75–0.96) confirmed that location identity accounted for the dominant share of variance in all indices. Climate and vegetation explained negligible fractions of the temporal trends: adding temperature, precipitation, and NDVI to the models caused no meaningful attenuation of the year coefficient for any index except abundance. LMMs offer substantial advantages over location-by-location regression, including partial pooling of information across sites, formal decomposition of variance between alpha and beta levels, and valid inference under the clustered structure of monitoring data.

Keywords: Breeding Bird Survey; biodiversity monitoring; linear mixed-effects models; alpha diversity; beta diversity; species richness; biotic homogenization; North America; long-term trends; climate effects.

Introduction. Biodiversity underpins ecosystem functioning, resilience, and the services that natural systems provide to human societies [1]. Quantifying how biodiversity changes over time and identifying the environmental drivers of such change are therefore central tasks of contemporary ecology and conservation biology. Yet biodiversity is not a single quantity – it is structured across spatial scales. The framework introduced by [7] distinguishes local (alpha) diversity, the diversity measured at a single site; regional (gamma) diversity, the diversity of a whole landscape or continent; and beta diversity, the variation in species composition among sites that connects alpha to gamma scales.

This multi-scale structure has important consequences for how biodiversity trends are analysed and interpreted. A gamma-level analysis – for example, counting the total number of species